NASA TECHNICAL MEMORANDUM 101675

AN EVALUATION OF THE PRESSURE PROOF TEST CONCEPT FOR THIN SHEET 2024-T3

D. S. Dawicke, C. C. Poe, Jr.,
J. C. Newman, Jr., and C. E. Harris

April 1990

National Aeronautics and
Space Administration

Langley Research Center
Hampton, Virginia 23665

AN EVALUATION OF THE PRESSURE PROOF TEST CONCEPT FOR THIN SHEET 2024-T3

D.S. Dawicke*, C.C. Poe, Jr.**, J.C. Newman, Jr.**, and C.E. Harris**

* Analytical Services and Materials, Inc., Hampton, VA 23666
** NASA Langley Research Center, Hampton, VA 23665

SUMMARY

The concept of pressure proof testing of fuselage structures with fatigue cracks to insure structural integrity was evaluated from a fracture mechanics viewpoint. A generic analytical and experimental investigation was conducted on uniaxially loaded flat panels with crack configurations and stress levels typical of longitudinal lap splice joints in commercial transport aircraft fuselage. The results revealed that the remaining fatigue life after a proof test was longer than that without the proof test because of crack growth retardation due to increased crack closure. However, based on a crack length that is slightly less than the critical value at the maximum proof test stress, the minimum assured life or proof test interval must be no more than 550 pressure cycles for a 1.33 proof factor and 1530 pressure cycles for a 1.5 proof factor to prevent in-flight failures.

INTRODUCTION

Several recent incidents involving fatigue cracking have raised concerns about the structural integrity of the aging commercial transport aircraft fleet. The development of multiple site damage (MSD) in lap-splice joints and other structural components is of great concern to the aerospace community. MSD is the formation of a row of cracks, such as along the top line of rivets in a lap-splice joint. The critical size of the individual cracks may be relatively small, making their detection with current nondestructive examination (NDE) methods difficult. The most well known incidence of a MSD failure involved an Aloha Airlines Boeing 737-200. This aircraft suffered a major structural failure resulting from MSD developing along the top row of rivets of a lap-splice joint, as shown in Figure 1.

The procedure of overpressurizing the fuselage of commercial transport aircraft has been postulated as a proof test that will insure the continued safe operation of aircraft with MSD fatigue cracks. A precedent for conducting the proof test at a pressure above the normal in-flight pressure exists because all new commercial transport aircraft are subjected to the design limit pressure certification of 1.33P, where P is the normal in-flight pressure. However, after certification the fuselage is only required to be fail-safe or damage tolerant at 1.10P. At no other time in the life of the airplane would the fuselage be subjected to the design limit pressure unless a major structural repair or alteration requires a new certification.

The strategy for evaluating the concept of pressure proof testing is based on the assumption that the proof test is an alternative to NDE to insure that critical fatigue cracks are not present in the fuselage. First, considering the principles of fracture mechanics and the ductile fracture behavior of 2024-T3 aluminum alloy, a fatigue crack will extend by stable tearing on each load cycle prior to reaching a critical crack length. When the critical crack length is reached, unstable or catastrophic crack extension will occur. Second, for the proof test to function as an alternative to NDE, the assumption must be made that after a successful test, defined as no catastrophic structural failure, cracks exist in the fuselage which are just smaller than the critical crack at the proof test stress. Given these two basic tenets, a proof test logic was established, as illustrated in Figure 2a. In this illustration, the proof test pressure was taken to be 1.33P (a proof factor of 1.33). At this pressure, the critical crack length, c_r, can be calculated using the crack growth resistance curve (R-curve) for 2024-T3 aluminum alloy that specifies the amount of stable tearing which will take place during the proof test. The minimum assured life of the fuselage is then determined by predicting the fatigue crack growth until the residual strength is degraded below the required value for the normal in-flight pressure. It should be noted that the actual remaining life must be defined as the life at which the residual strength degrades below the 1.10P fail-safe pressure. This requirement was not used because the actual residual strength could not be checked while cycling at the 1.0P stress in the experimental verification tests. Therefore, the reported lives are slightly higher than the actual minimum assured fatigue lives.

The residual strength of the fuselage will, at least initially, be decreased by a single proof test cycle, as shown in Figure 2a. However, the net effect of the proof test is to increase fatigue life as a result of the crack growth retardation resulting from elevated crack closure due to the proof cycle, as shown in Figure 2b. The amount of increase in fatigue life is a function of proof factor, operational pressure level, and crack length.

The technical evaluation of the concept of pressure proof testing components with MSD is summarized in this paper. Proof test simulations were conducted on flat center crack tension (CCT) specimens, multiple-open hole specimens, and riveted lap-splice joint specimens, which are illustrated in Figure 3. Fatigue life predictions were made using a fatigue crack closure model [1] with verification derived from comparisons with experiments. The generic experimental and analytical investigation was conducted for several issues considered to be critical for making the decision to employ proof testing. However, all of the issues that must be considered in proof testing fuselage structures could not be technically evaluated because NASA has neither the resources nor access to fuselage design details and stress analyses of the jet transports in the

commercial fleet. The conclusions stated herein are based solely on the technical results of the subject evaluation as reported in this document.

EXPERIMENTS

The experiments conducted in the proof test evaluation were intended to simulate the effect of a proof test on a typical commercial transport aircraft fuselage material and structural configuration. The structural configuration examined was a riveted lap-splice joint. Tests were conducted on flat uniaxially-loaded CCT specimens, multiple-open hole specimens, and lap-splice specimens with a single row of rivets. The specimen configurations were chosen to provide a progression of increasingly more complex configurations and bring into account the important structural details of MSD and rivet-loading, while at the same time maintaining the simplicity of coupon specimens. The operational stress levels were in the range of 10-14 ksi, which are typical of the levels present in fuselage skins. The actual fuselage structures are curved, supported by other load carrying structures (such as tear straps and stringers), and subjected to pressure loading which results in biaxial stresses in the fuselage skin. These details were not examined in this evaluation.

The proof tests were conducted by first precracking, from an initial saw cut(s) of half length c_n, to obtain natural cracks. The specimens were then loaded under stroke control until the onset of maximum load (unstable crack extension under load control). If the specimen survived the proof cycle, the crack would have been slightly less than critical. The fatigue (or operational) stress was obtained by dividing the proof stress by the proof factor. The specimens were then cycled at the operational stress until failure (minimum stress equal to zero). The half crack length at failure (c_f) was recorded.

The desired operational stress range was obtained by estimating the crack length (c_r) which would result in a near critical crack for the given proof conditions. The 2024-T3 aluminum alloy fractures at about net section-yield stress equal to the yield stress, making the critical crack length estimation very simple. Some of the proof tests were followed by fatigue tests which had the same initial crack length and operational stress, but had no proof cycle applied These tests served to define the increase in life due to beneficial crack-growth retardation from the proof stress. The following sections provide details of the proof and fatigue tests for each of the three specimen configurations.

Center Crack Tension Specimens

The CCT specimens were intended to describe the effect of the proof test on a single crack in a fuselage structure. This configuration also represents a case of MSD, because the stress intensity factor solution for a center crack in a finite plate is nearly identical to the solution for a linear array of equal length cracks.

Proof and fatigue tests were conducted on 12 and 3 inch wide CCT specimens with thicknesses of 0.050, 0.063, and 0.071 inches, as summarized in Table 1. Two operational stress levels were examined for a proof factor of 1.33. The low stress level (10-14 ksi) resulted from initial half-crack lengths of 4 inches in 12 inch wide specimens. The high stress level (23-27 ksi) resulted from initial half crack lengths of 2 inches in 12 inch wide specimens and 0.5 inch initial half-crack length in 3 inch wide specimens. One additional test was conducted at a 1.5 proof factor.

The crack lengths were measured optically and evaluated from the unloading compliance behavior determined from centerline displacement measurements. Localized buckling at the crack plane was prevented by using thick guide plates placed on both sides of the specimen to restrict out of plane motion. The guide plates had a 0.5 inch by 11 inch long slot for viewing the crack.

The critical crack length was estimated, for a given proof factor and operational stress range, assuming a net section stress failure criterion. Failure of the 12 inch wide CCT specimens occurred at net-section stresses of 48 ksi, with the net-section stress calculations based on the uncracked area prior to loading. The centerline displacement was monitored during the application of the displacement-controlled proof stress. A plot of the displacement as a function of stress was linear for low stresses, but the displacement increased rapidly as the maximum (or critical) stress was approached. The critical stress was taken to be the point at which the slope of the stress against load-line displacement curve became nearly zero. A further increase in the applied displacement would have resulted in a reduction in the applied stress.

Multiple-Open Hole Specimens

The multiple-open hole configuration was intended to represent a slightly more complex case of MSD. This configuration simulates the effect of proof and fatigue loading on a linear array of cracks propagating from open holes spaced one-inch apart.

Fatigue tests, with and without a proof cycle, were conducted on 11.8 inch wide multiple-open hole specimens with thicknesses of 0.050 and 0.071 inches, as summarized in Table 2. Each specimen had ten, 3/16 inch diameter holes aligned in a row perpendicular to the loading direction. The holes were spaced an inch apart and notched on both sides to promote the crack development. Crack lengths were measured optically and, again, buckling was prevented using the same guide plates as used for the CCT specimens. All proof tests were conducted at a 1.33 proof factor.

Initially, the equivalent critical crack length (summation of the 10 cracks and holes) was estimated in the same manner as used in the CCT specimens. However, these specimens exhibited much less crack extension during the proof than the CCT specimens,which made it difficult to determine the critical condition. The proof cycle was applied under stroke control, but unlike the CCT specimens, rapid fracture occurred before the test could be terminated. The evaluation of the initial multiple-open hole tests revealed that failure occurred at a net section stress, based on the uncracked area prior to loading, of 44 ksi. Subsequent multiple-open hole specimens were then proof loaded to a net-section stress of 42-43 ksi. Thus, the cracks remaining in the specimens could be somewhat less than critical.

Three fatigue tests (no proof cycles) were also conducted for the same operational stress levels and total initial crack lengths as those in the proof tests. However, the individual distributions of cracking varied from test to test as it was difficult to duplicate exact cracking patterns during precracking.

Riveted Lap-Splice Joint Specimens

The riveted lap-splice joint configuration was intended to represent MSD in a structural component. However, structural elements, such as stiffeners, were not included in order to maintain the simplicity of coupon specimens. A single row of rivets was used to further simplify the analysis of the joint. However, the single row of rivets develop larger amounts of bending than that expected in multiple rows of rivets.

Fatigue tests, with a single proof cycle, were conducted on 12 inch wide riveted lap-splice joint specimens with thicknesses of 0.050 and 0.071 inches, as summarized in Table 3. Each specimen had ten, 3/16 inch diameter riveted holes aligned in a row perpendicular to the loading direction. The holes were spaced one-inch apart and notched on both sides to, again, promote the crack development. The crack lengths were measured optically. Out of plane bending was restricted by using guide plates. However, intense local out of plane rivet rotation was observed through the slots in the guide plates.

Each specimen was initially precracked as a multiple-open hole specimen. The specimen was then cut 2 inches above the holes, the two pieces overlaid, matched drilled, and riveted with button head rivets. Precracking was continued until the total critical crack length (summation of the 10 cracks) was obtained. As with the open hole specimens, small crack extensions during proof made the estimation of maximum load from the load-stroke curve difficult. Evaluation of the initial riveted lap-splice specimens revealed that failure occurred at a net-section stress, based on the uncracked area prior to loading, of 29 ksi. The subsequent riveted lap-splice specimens were loaded to a net-section stress of 27-28 ksi. One test (A2-07) was conducted at an initial crack length and stress level which was much less than critical.

ANALYSIS

The life predictions for the fatigue tests, with and without the proof cycles, conducted on the CCT, multiple-open hole, and riveted lap-splice joint specimens were made using a plasticity-induced crack closure model [1]. The model was based on Elber's crack closure phenomenon [2-3] and the Dugdale plastic-zone model [4]. Elber observed that fatigue cracks close at loads above the minimum load, reducing the stress intensity factor range over which damage occurs, as illustrated in Figure 4. The reduced stress intensity factor range was called the "effective stress intensity factor range" (ΔK_{eff}). The closure behavior was attributed to the development and contact of a region of plastically deformed material behind the crack tip (crack wake) resulting from the crack propagating through the plastic zone, as illustrated in Figure 4.

At the high stress levels examined in this study, the plastic zone is no longer small compared to the crack length, making linear-elastic analyses inadequate. The Dugdale plastic zone length (ρ) was added to the crack length (c) to correct for plasticity effects, in the same manner as the Irwin plastic zone correction. The plasticity corrected effective stress intensity factor (ΔK_{eff}) [5] becomes:

$$\Delta K_{eff} = (S - S_o)\sqrt{\pi d}\, F(d/w) \qquad (1)$$

where S is the maximum fatigue stress, S_o is the crack opening stress, d is the sum of the crack and plastic zone lengths, w is the specimen half width and F(d/w) is the boundary correction factor. The effective stress intensity factor was defined in terms of the current crack length (including the current crack growth increment) to model stable crack growth during proof. An infinite periodic

array of Dugdale models [6] as modified in references 5 and 7 was used to determine the plastic zone length as:

$$\rho = c\left\{(2w/\pi c)\sin^{-1}\left[\sin(\pi c/2w)\sec(\pi Sf/2\alpha\sigma_o)\right] - 1\right\} \quad (2)$$

$$f = 1 + 0.22(c/w)^2 \quad (3)$$

The flow stress (σ_o) is the average between the yield (52 ksi) and ultimate (71 ksi) tensile strength. The constraint factor (α) is an assumed elevation factor on the flow stress that develops at the crack tip due to three-dimensional stress states. Additional details of the crack closure model are presented in references 1 and 8.

Stress intensity factor solutions were established for the configurations used in the experimental portion of the study, as given in Appendix A. The stress intensity factor for the CCT specimens had a finite width correction factor. The stress intensity factors for the multiple-open hole and riveted lap-splice specimens were based on a solution for an infinite linear array of cracks under various loading [6,9].

The crack growth rate description was developed from baseline data covering nine orders of magnitude, including the threshold regime (10^{-7} to 10^{-9} inch/cycle) [10], the mid-rate regime (10^{-3} to 10^{-7} inch/cycle) [11], the high-rate regime (>10^{-3} inch/cycle) [12], and additional high growth rate data from R-curve tests. The use of the plasticity corrected effective stress intensity factor range correlated all of the crack growth rate data, including that from the R-curve tests, as shown in Figure 5.

The R-curve data was included with the crack growth rate data by treating the stable crack extension as the crack growth in one cycle. The plasticity corrected effective stress intensity factor is similar to K_R because the crack opening stresses developed during the fatigue precracking process of the R-curve test are very small. An expanded view of the upper portion of the crack growth data is shown in Figure 6, illustrating the correlation between the R-curve and fatigue crack growth rate data.

A life prediction based on the crack closure analysis was made for each test conducted in the experimental portion of the study. The MSD cracking of the multiple-open hole and riveted single lap-splice specimens was analyzed by assuming an average crack length (equal cracking at each hole). The riveted lap-splice joint tests had local bending present elevating the crack tip stresses. The stress intensity factor was modified by multiplying the applied stress in the stress

intensity factor solution by $(1 + \gamma/2)$, where γ is the ratio of the outer fiber bending stress to the axial stress [13].

RESULTS AND DISCUSSION

The closure based life predictions were compared with the experimental results for each of the three configurations. Minimum assured lives were obtained for the fatigue tests with a single proof cycle and other conditions not addressed experimentally. The minimum assured lives were used to examine the effect of the proof cycle interval on the life of non-critical cracks.

Center Crack Tension Specimens

A comparison of the closure based life predictions and the experimental results from the CCT specimen proof and fatigue tests is given in Table 4. The predicted fatigue lives, crack extension during the proof (or first fatigue) cycle, and final crack length are presented in terms of the ratio of predicted to experimental values. The average ratio of predicted-to-test life was 1.06 with a standard deviation of 0.33. The average ratio of predicted-to-test crack extension was 0.96 with a standard deviation of 0.3. Crack lengths at failure were predicted within 5% of the test values.

The measured and predicted crack length against cycle behaviors of two CCT fatigue tests, one with and one without a proof cycle, are presented in Figure 7a. The predictions agreed well with the experimental data for both crack extension during the proof cycle and total fatigue life. The predicted lives were 0.73 of the experimental values for the tests with the single proof cycle and 1.21 of the experimental value for the tests without the proof cycle. The predicted and measured crack opening stresses for the same two tests are shown in Figure 7b. The crack opening stresses were measured from a displacement gage placed along the centerline of the crack. The predicted crack opening values for the proof test agreed well with the measurements, while those from the fatigue tests tended to be lower than the measured values. The remote displacement gage tended to give more distinct measurements of crack opening after the proof cycle.

The effects of the proof cycle and proof factor on fatigue life of CCT specimens are shown in Figure 8 for tests conducted at operational stress levels around 11.5 ksi. The tests conducted with a 1.33 proof factor resulted in an average minimum assured life of 146 cycles, which was almost 3 times the life of identical tests conducted without the proof cycle. The large difference in

lives was a result of beneficial crack growth retardation due to the single proof cycle. The predicted fatigue lives were higher than that obtained from the actual tests (but within a factor of 1.3). A single test was conducted at a proof factor of 1.5 and resulted in a fatigue life of 604 cycles, over 4 times the life of the tests conducted at the 1.33 proof factor. The predicted results gave508 cycles to failure. (The predicted life without the proof was larger than that given for the 1.33 proof factor because the initial crack length was smaller).

The tests and analysis indicates that the application of a proof cycle (1.33 proof factor) triples the remaining fatigue life of a CCT specimen. However, the crack extension during proof takes up about 40% of the total crack growth prior to failure and the prediction of this extension is crucial to accurate life predictions.

Multiple-Open Hole Specimens

The length of the cracks at each hole was measured before the application of the proof cycle, after the proof cycle and at several intervals prior to failure. Four of the tests had unequal cracking resulting in crack link-up prior to the application of the proof cycle. These tests experienced additional crack link-ups prior to failure, as shown for specimen A2-06 in Figure 9. The specimen had been precracked prior to the application of the proof cycle, during which cracks of 2 holes linked-up (holes 4 and 5). The numbers below each hole indicate the total crack length (2c) in inches. The proof cycle caused crack extensions at nearly every hole, with the greatest extensions for the longest cracks. Subsequent operational cycles caused additional crack link-up and crack extensions, as shown by the crack distribution at cycles 100, 200, and 500 of Figure 9. The other five tests had nearly equal cracking before and after the proof cycle, with failure resulting shortly (1 to 20 cycles) after the first occurrence of crack link-up. The distribution of cracks among the ten holes varied from test to test, as seen in Figure 10 for the patterns prior to the application of the proof cycle or before the first fatigue cycle.

A comparison of the closure based life predictions and the experimental results on the multiple-open hole specimen tests is given in Table 5. Life predictions were made for each of the following assumed crack configurations: a linear array of equal length cracks (average before proof or first fatigue cycle), a single center crack whose length is the sum of the ten individual cracks, and a linear array of equal length cracks based on the crack sizes after the proof. The average crack length based life predictions tended to predict lives longer than observed experimentally for tests, especially for specimens with unequal cracking and crack link-up. The analysis based on a single large crack produced life predictions within 17% of the experimental values for the two tests which had large dominant cracks (A1-11 and A2-08), but was overly

conservative for the tests with more equal cracking. Test A1-04 had major crack link-up during the proof and was not predicted well by any of the methods.

The most significant shortcoming of the current analysis is the inability to describe unequal cracking and crack link-up. The assumption of equal cracking may not be the most critical case and as a result, the predicted lives tended to be longer than observed experimentally. This is best illustrated by examining the crack length against cycle behavior of tests A2-33 and A2-34, as shown by the symbols in Figure 11. These two tests had nearly the same initial total crack length and loading conditions, but one lasted 372 cycles while the other lasted 501 cycles. The closure based life prediction, shown as the solid line in Figure 11, follows the behavior of the experimentally measured crack lengths up to the point of link-up of the longest cracks. The sudden increase in crack length caused rapid crack extension and failure within the next 2 cycles. The analysis currently cannot predict this type of failure mode due to the assumption of equal cracking at each hole. Crack link-up prior to the proof presents a different type of problem for the analysis. The link-up of two or more cracks greatly increases the stress intensity factor of the linked-up crack, which results in large crack extensions during proof and high crack growth rates in fatigue, as shown in Figure 12. The solid symbols of Figure 12 represent the average measured crack lengths and the solid line is the closure based life prediction based on the average crack length prior to proof.

The analysis indicated that accurate description of the specific crack configurations are required for accurate MSD life predictions. Simple approximations of the cracking pattern cannot provide useful bounds for every MSD cracking configuration. It is believed that a fracture mechanics approach, tracking individual cracks and accounting for crack interaction and link-up could predict crack growth behavior of MSD cracking, as shown by the life predictions made with stress intensity factor solutions which reflect the specific cracking distribution.

Riveted Lap-Splice Joint Specimens

Again, the crack length for each hole was measured before the application of the proof stress, after the proof stress and at several intervals during the test. Some typical results are shown in Figure 13 for a fatigue test with a single proof cycle. The distribution of cracks among the ten riveted holes varied from test to test, as seen in Figure 14 for the patterns prior to and following the application of the proof cycle. The longest crack dominated the crack growth and became critical through link-up with adjacent cracks.

The riveted lap-splice joints were tested with guide plates to prevent buckling and out-of-plane bending. However, localized bending was observed along the row of rivets and life predictions which neglected bending produced longer lives than were observed experimentally. A simple strength of materials estimation of bending, neglecting the contribution of the guide plates, indicated that the parameter describing the elevation of stresses (γ) should be 3. Two tests (A2-31 and A2-32) had severe bending present along the row of rivets, while other tests (A1-12, A2-05, A2-37 and A2-38) had noticeably less bending. A comparison of the closure based life predictions and the experimental results on the riveted lap-splice joint is given in Table 6.

The life predictions for three riveted lap-splice joint specimens with various amounts of rivet bending is shown in Figures 15-17. The different levels of bending was obtained through changing the amount of rivet compaction and increasing the effectiveness of the guide plates. The severity of bending was based on observations of the local out-of-plane rivet rotations and deformations during the tests. All three tests had nearly the same initial total crack length, proof factor, and operational fatigue stress, yet the lives ranged from 160 to 2460 cycles. Predictions of the crack growth behavior were made assuming both no bending ($\gamma = 0$) and a strength of materials estimate of the amount of bending present ($\gamma = 3$). The prediction with $\gamma = 3$ agreed with the experimental measurements for the test with severe bending (A2-31) until the rivets failed, as shown in Figure 15. The prediction with no bending ($\gamma = 0$) agreed with the experimental measurements for the test which exhibited very little bending (A2-37) until first crack link-up occurred, as shown in Figure 16. The crack growth behavior of the specimen which exhibited moderate bending fell between the no bending ($\gamma = 0$) and severe bending ($\gamma = 3$) predictions, as shown in Figure 17.

Analysis of MSD with Equal Spaced Cracks

Critical Cracks. The extent of crack growth retardation observed in the multiple-open hole and riveted lap-splice joint MSD experiments and predictions was less than that observed in the CCT specimens. Direct experimental comparison of life with and without the proof cycle was not possible in the multiple-open hole or riveted lap-splice specimens because exact crack distributions could not be duplicated. However, the direct comparison could be made with the analysis, as shown in Figure 18. The analysis assumed equal crack lengths at each hole for the multiple-open hole and riveted configurations and considered the crack length just critical at the application of the proof stress. At an operational stress of 1P=12 ksi, the crack growth retardation due to the single 1.33 proof cycle resulted in a life twice as long as the test without the proof cycle for the CCT configuration, while the increase in life was only 1.5 times for the multiple-open hole and riveted configurations.

The fatigue crack closure analysis was used to examine other operational conditions not addressed experimentally. The analysis considered the riveted lap-splice configuration and varied the proof factor and operational stress level to observe their effect on the cycles to failure, as shown in Figure 19. No bending was considered in the analysis and equal cracking at each rivet hole was assumed. In each case, the initial crack length was chosen to be just critical during the application of the proof cycle. The predicted cycles to failure increased as the proof factor increased and/or the operational stress decreased. The values given in Figure 19 represent the minimum assured life for the various operational conditions. To determine a safe proof test interval, the indicated minimum assured lives would have to be divided by an appropriate safety factor.

Non-Critical Cracks. The effect of multiple proof cycles on the life of non-critical cracks was examined for the riveted lap-splice joint configuration. The fatigue crack closure model was used to predict the cycles to failure of non-critical cracks based on the assumption of equal crack lengths at every rivet. The initial crack lengths examined ranged from 80 to 100% of the crack length just critical at the proof stress (c_r). The critical crack lengths at proof were calculated using the Two Parameter Fracture Criterion [14] and found to be 0.376 and 0.359 inches for the 1.33 and 1.5 proof factors, respectively. The minimum assured lives for a fatigue test with a single proof cycle was 550 and 1530 for proof factors of 1.33 and 1.5 respectively. Thus, the proof cycles were applied at the first cycle and repeated every 550 cycles for the 1.33 proof factor, and every 1530 cycles for the 1.5 proof factor. Proof cycle intervals of 1000 and 2000, for the 1.33 and 1.5 proof factors respectively, were also analyzed to examine the effect of choosing too large of a proof cycle interval. The 1P operational stress was 12 ksi, no bending was considered, and equal cracking at each hole was assumed in the analysis. The life without any proof cycles was also predicted. The predicted lives, in terms of cycles to failure as a function of the initial crack length normalized to the crack length just critical under the proof cycle (c_i/c_r), are shown in Figures 20 and 21 for the 1.33 and 1.5 proof factors, respectively.

The crack length against life behavior for a successful proof factor and proof cycle interval combination appears as a series of step functions, indicating that failure occurs only during the application of a proof cycle. This type of behavior is seen in Figure 20 for the 1.33 proof factor applied every 550 cycles and in Figure 21 for the 1.5 proof factor applied every 1530 cycles. If the interval between applications of the proof stresses is too large, then it would be possible to have an in-flight failure between applications of the proof cycles. This type of behavior is indicated as the small dashed lines in Figure 20 for the 1.33 proof factor applied every 1000 cycles and in Figure 21 for the 1.5 proof factor applied every 2000 cycles. The predicted cycles to failure

for the proof test interval based on the minimum assured life follows the trend of the predicted cycles to failure for the fatigue test without any proof cycles (the large dashed curves of Figures 20 and 21). This indicates that for crack lengths near critical, the multiple interval proof test does not provide substantial increases in life. However, as the initial crack length decreases, the retardation of the proof cycles does provide an increase in life.

CONCLUDING REMARKS

The concept of pressure proof testing of fuselage structures with fatigue cracks to insure structural integrity was evaluated from a fracture mechanics viewpoint. A generic investigation was conducted on the behavior of uniaxially-loaded, unstiffened flat panels with crack configurations and stress levels typical of the longitudinal lap splice joints in the fuselage of commercial transport aircraft. The specific conclusions from this investigation are as follows:

1. The remaining fatigue life with a proof cycle is longer than that without the proof cycle because of the effect of crack growth rate retardation.

2. The remaining life after the proof cycle increases with increasing proof factor and also increases with decreasing normal operating pressure for a constant proof factor.

3. Fatigue life calculations from the crack-closure model agreed well with tests on center crack tension specimens (mean of ratio of predicted-to-test life on center crack tension specimens was 1.06 with a standard deviation of 0.33).

4. The prediction of MSD fatigue crack growth behavior is strongly dependent upon accurate stress intensity factor descriptions of specific cracking patterns. The current analysis can describe the behavior for equal cracking, but cannot describe unequal cracking and crack link-up.

5. The proof test interval can be no more than 550 pressure cycles for a proof factor of 1.33 and 1530 pressure cycles for a proof factor of 1.5 to prevent in-flight failures. These values may be unconservative due to the possibility of unequal cracking and crack link-up, and also because nominal material property values were used in the analysis.

6. In-flight failures are possible if the proof test interval is too large.

The decision to conduct a pressure proof test of the fuselage cannot be made solely on the basis of this investigation because all aspects of the problems were not considered. For example, a proof test produced by cabin pressure will not result in the critical stress state in several regions of the fuselage structure. Furthermore, the possibility of developing critical cracks in the components of the fuselage stiffener system such as window frames, circumferential frames, longitudinal stiffeners, and the aft pressure bulkhead must be evaluated. Finally, the results of this

investigation may not be conservative because the effects of corrosion on the measured and predicted fatigue lives were not addressed.

REFERENCES

[1] Newman, J.C., Jr., "A Crack Closure Model for Predicting Fatigue Crack Growth Under Aircraft Spectrum Loading," *Methods and Models for Predicting Fatigue Crack Growth Under Random Loading*, ASTM STP 748, 1981, pp. 53-81.

[2] Elber, W., "Fatigue Crack Closure Under Cyclic Tension," *Engineering Fracture Mechanics*, Vol. 2, No. 1, 1970, pp. 37-45.

[3] Elber, W., "The Significance of Fatigue Crack Closure," *Damage Tolerance in Aircraft Structures*, ASTM STP 486, 1971, pp. 230-242.

[4] Dugdale, D.S., "Yielding of Steel Sheets Containing Slits," *Journal of the Mechanics and Physics of Solids*, Vol. 8, No. 2, 1960, pp. 100-104.

[5] Newman, J.C., Jr., "A Nonlinear Fracture Mechanics Approach to the Growth of Small Cracks," *Behavior of Short Cracks in Airframe Components*, AGARD CP-328, 1982, pp. 6.1-6.26.

[6] Smith, E.,"Fracture at Stress Concentrations," Proceedings from the First International Conference on Fracture, 1965, pp. 139-151.

[7] Newman, J.C., Jr., ASTM STP 896, 1985, pp. 139-166.

[8] Newman, J.C., Jr., Poe, C.C., Jr., and Dawicke, D.S., "Proof Test and Fatigue Crack Growth Modeling on 2024-T3 Aluminum Alloy, Submitted for Publication at FATIGUE 90, the Forth International Conference on Fatigue, 1990.

[9] Newman, J.C., Jr., "Predicting Failure of Specimens with Either Surface or Corner Cracks at Holes," NASA TN D-8244, 1976.

[10] Phillips, E.P, "The Influence of Crack Closure on Fatigue Crack Growth Thresholds in 2024-T3 Aluminum Alloy," *Mechanics of Fatigue Crack Closure*, ASTM STP 982, 1988, pp. 505-515.

[11] Hudson, C.M., "Effect of Stress Ratio on Fatigue-Crack Growth in 7075-T6 and 2024-T3 Aluminum Alloy Specimens," NASA TND-5390, 1969.

[12] Dubensky, R.G., "Fatigue Crack Propagation in 2024-T3 and 7075-T6 Aluminum Alloys at High Stresses," NASA CR-1732, 1971.

[13] Roberts, R. and Erdogan, F., "The Effect of Mean Stress on Fatigue Crack Propagation in Plates Under Extension and Bending," *Journal of Basic Engineering*, 1967, pp. 885-892.

[14] Newman, J.C., Jr., "Fracture Analysis of Various Cracked Configurations in Sheet and Plate Materials," *Properties Related to Fracture Toughness*, ASTM STP 605, 1976, pp. 104-123.

[15] Tada, H., Paris, P.C., and Irwin, G.R., *The Stress Analysis of Cracks Handbook*, Del Research Corporation, 1973.

APPENDIX A: STRESS INTENSITY FACTOR SOLUTIONS

Stress intensity factor solutions were established for each of the specimen configurations used in the experimental portion of the study.

Center Crack Tension Specimen

The stress intensity factor for the CCT specimen used the secant finite width correction factor [15].

$$K = S\sqrt{\pi c \sec\left(\frac{\pi c}{2w}\right)} \tag{A1}$$

where:

K = stress intensity factor
S = applied stress
c = half crack length
w = half width

Multiple-Open Hole Specimen

The stress intensity factor for the open hole specimen took into account adjacent cracks by defining the half width (w) as half of the distance between the center lines of two adjacent holes [6,9].

$$K = S\sqrt{2w \tan\left(\frac{\pi c}{2w}\right)\,(1 - r/c)\,F\left(\frac{r}{c}\right)} \tag{A2}$$

$$F(x) = 1.0 + 0.358x + 1.425x^2 - 1.578x^3 + 2.156x^4 \tag{A3}$$

where:

r = hole radius
x = r/c

Riveted Lap-Splice Specimen

The stress intensity factor for the riveted lap-splice specimen was based on the pin-loaded solution with a constant (γ) to elevate the stress due to the estimated bending present [6,9].

$$K = S\left(1 + \gamma/2\right)\left(0.5 + \frac{1}{2\sin\left(\pi c/2w\right)}\right)\sqrt{\pi c \frac{\sin\left(\pi c/2w\right)}{\cos\left(\pi c/2w\right)}\left(1 - \pi c/2w\right)}\;F\left(\frac{r}{c}\right) \tag{A4}$$

Table 1
Experimental CCT Proof and Fatigue Results

Specimen ID	t (inch)[a]	w (inch)[a]	Precrack S_{max}[b] (ksi)	c_n (inch)[c]	c_i (inch)[c]	Proof S_{max} (ksi)	Proof Δc (inch)	Fatigue S_{max}[b] (ksi)	Cycles to Failure	c_f (inch)[c]
A3-01	0.063	6.0	---[d]	1.996	1.996	33.7	0.394	25.3	103	3.224
A3-02	0.063	6.0	---[d]	1.988	1.988	---	---	25.0	47	3.205
A3-03	0.063	6.0	---[d]	4.000	4.000	16.1	0.220	12.2	101	4.705
A3-04	0.063	6.0	---[d]	3.988	3.988	---	---	12.3	37	4.665
A3-05	0.063	6.0	4.0	1.752	2.000	---	---	25.0	63	3.106
A3-06	0.063	6.0	2.2	3.750	4.000	---	---	12.4	47	4.472
A3-07	0.063	6.0	2.2	3.750	3.996	15.3	0.185	11.5	211	4.626
A1-01	0.071	5.9	3.7	1.750	1.999	---	0.059[e]	24.4	47	3.079
A1-03	0.071	5.9	3.7	1.750	2.001	32.5	0.484	24.4	114	3.217
A1-05	0.071	5.9	2.0	3.750	3.997	---	0.024[e]	11.4	57	4.567
A1-09	0.071	5.9	2.0	3.750	3.999	15.1	0.311	11.4	109	4.610
A1-13	0.071	5.9	2.1	3.500	3.750	17.3	0.528	11.5	604	4.665
A2-09	0.050	5.9	2.0	3.750	4.000	15.7	0.197	11.8	117	4.567
A2-22	0.050	1.5	7.4	0.375	0.499	35.0	0.033	26.4	782	0.815
A2-27	0.050	1.5	7.4	0.375	0.500	---	0.007[e]	26.4	266	0.898
A2-30	0.050	1.5	26.5	0.375	0.510	35.0	0.008	26.4	542	0.823

Note:

[a] w is the specimen half width t is the specimen thickness.

[b] The minimum precrack and fatigue stress was zero.

[c] The crack lengths c_n (notch length), c_i (initial crack length), and c_f (final crack length) are half crack lengths.

[d] No precracking, a sawcut was used as initial crack.

[e] Crack extension during first cycle of fatigue test (no proof stress applied in tests).

Table 2
Multiple-Open Hole Proof and Fatigue Test Results

Specimen ID	t (inch)[a]	w (inch)[a]	Precrack S_{max}[c] (ksi)	c_n (inch)[b]	c_i (inch)[b]	Proof S_{max} (ksi)	Proof Δc (inch)	Fatigue S_{max}[c] (ksi)	Cycles to Failure
A1-04	0.071	5.9	10.0	0.12	0.3678	12.6	0.039	9.5	305
A1-11	0.071	5.9	10.0	0.12	0.3432	16.5	0.021	12.4	298
A2-06	0 050	5.9	10.0	0.12	0.3276	18.7	0.008	14.0	541
A2-08	0.050	5.9	10.0	0.12	0.3615	14.3	0.016	10.7	463
A2-02	0.050	5.9	10.0	0.12	0.3277	---	---	14.0	1096
A2-10	0.050	5.9	10.0	0.12	0.3276	---	---	14.0	298
A2-13	0.050	5.9	14.0	0.12	0.3276	---	---	14.0	1269
A2-33	0.050	5.9	10.0	0.12	0.3221	18.6	0.020	13.9	372
A2-34	0.050	5.9	10.0	0.12	0.3243	18.6	0.053	13.9	501

Note: [a] w is the specimen half width and t is the specimen thickness.
[b] The crack lengths c_n (notch length) and c_i (initial crack length) are the average (of the 10 holes) half crack lengths.
[c] The minimum precrack and fatigue stress was zero.

Table 3
Riveted Lap-Splice Proof Tests Results

Specimen ID	t (inch)[a]	w (inch)[a]	Precrack S_{max}[c] (ksi)	c_n (inch)[b]	c_i (inch)[b]	Proof S_{max} (ksi)	Proof Δc (inch)	Fatigue S_{max}[c] (ksi)	Cycles to Failure
A1-12	0.071	5.9	10.0	0.12	0.3497	12.9	0.018	9.7	563
A2-05	0.050	5.9	10.0	0.12	0.3495	14.0	0.018	10.5	1182
A2-31[d]	0.050	5.9	10.0	0.12	0.3003	14.4	0.078	10.8	160[e]
A2-32[d]	0.050	5.9	10.0	0.12	0.3160	14.3	0.056	10.8	59[e]
A2-37	0.050	5.9	10.0	0.12	0.2986	13.7	0.066	10.3	2460
A2-38	0.050	5.9	10.0	0.12	0.3012	13.7	0.006	10.3	1523

Note: [a] w is the specimen half width t is the specimen thickness.
[b] The crack lengths c_n (notch length) and c_i (initial crack length) are the average (of the 10 holes) half crack lengths.
[c] The minimum precrack and fatigue stress was zero.
[d] Severe bending present along the row of rivets.
[e] Rivet failure occured before fatigue failure.

Table 4
Fatigue Crack Growth Predictions for the CCT Proof and Fatigue Tests

Specimen ID	c_i (inch)	w (inch)	Fatigue S_{max} (ksi)	Proof Factor	Cycles to Failure N_t	Ratio of Predicted to Test: Cycles to Failure N_p/N_t	Ratio of Predicted to Test: Proof $\Delta c_p/\Delta c_t$	Ratio of Predicted to Test: Crack Length at Failure c_p/c_t
A3-01	1.996	6.0	25.3	1.33	103	1.11	1.0[a]	0.94
A3-02	1.988	6.0	25.0	1.00[b]	47	1.17	----	0.96
A3-03	4.000	6.0	12.2	1.33	101	1.53	1.0[a]	0.99
A3-04	3.988	6.0	12.3	1.00[b]	37	1.50	----	0.99
A3-05	2.000	6.0	25.0	1.00[b]	63	0.80	----	0.98
A3-06	4.000	6.0	12.4	1.00[b]	47	1.00	----	1.04
A3-07	3.996	6.0	11.5	1.33	211	1.57	1.01	1.02
A1-01	1.999	5.9	24.4	1.00[b]	47	1.21	1.09	1.00
A1-03	2.001	5.9	24.4	1.33	114	0.73	1.03	0.95
A1-05	3.997	5.9	11.4	1.00[b]	57	1.31	1.53	1.02
A1-09	3.999	5.9	11.4	1.33	109	1.36	0.83	1.01
A1-09	3.999	5.9	11.4	1.33	109	0.90	1.0[a]	1.01
A1-13	3.750	5.9	11.5	1.50	604	0.84	0.63	0.97
A2-09	4.000	5.9	11.8	1.33	117	0.99	1.24	1.01
A2-22	0.499	1.5	26.4	1.33	782	0.74	0.89	1.04
A2-27	0.500	1.5	26.4	1.00[b]	266	0.65	0.44	0.94
A2-30	0.510	1.5	26.4	1.33	542	0.53	0.95	1.01

Note: [a] The crack extension (Δc) was input in analysis to match test.
[b] A proof factor of 1.00 indicates only fatigue loading.

Table 5
Fatigue Crack Growth Predictions for the Multiple-Open Hole Proof and Fatigue Tests

Specimen ID	c_i (inch)	w (inch)	Fatigue S_{max} (ksi)	Proof Factor	Cycles to Failure N_t	Ratio of Predicted to Test: Method A N_p/N_t	Ratio of Predicted to Test: Method B N_p/N_t	Ratio of Predicted to Test: Method C N_p/N_t
A1-04	0.3678	5.9	9.5	1.33	305	7.78	3.08	0.27
A1-11	0.3432	5.9	12.4	1.33	298	4.14	1.17	1.19
A2-06	0.3276	5.9	14.0	1.33	541	1.77	0.51	1.39
A2-08	0.3615	5.9	10.7	1.33	463	3.00	1.05	1.37
A2-02[b]	0.3277	5.9	14.0	1.00[a]	1096	0.52	0.14	----
A2-10[b]	0.3276	5.9	14.0	1.00[a]	298	1.92	0.50	----
A2-13[b]	0.3276	5.9	14.0	1.00[a]	1269	0.59	0.14	----
A2-33[b]	0.3221	5.9	13.9	1.33	372	3.45	0.85	3.31
A2-34[b]	0.3243	5.9	13.9	1.33	501	2.37	0.65	2.32

Note: [a] A proof factor of 1.00 indicates only fatigue loading.
[b] Tests with near equal length cracks
Method A Linear array based on the average crack length before proof
Method B Single center crack
Method C Linear array based on the average crack length after proof

Table 6
Fatigue Crack Growth Predictions for the Riveted Lap-Splice Proof Tests

Specimen ID	c_i (inch)	w (inch)	Fatigue S_{max} (ksi)	Proof Factor	Cycles to Failure N_t	Ratio of Predicted to Test	
						Method A N_p/N_t	Method B N_p/N_t
A1-12	0.3497	5.9	9.7	1.33	563	7.41	0.37
A2-05	0.3495	5.9	10.5	1.33	1182	2.37	0.12
A2-31[a,b]	0.3003	5.9	10.8	1.33	160[c]	38.8	1.21
A2-32[a,b]	0.3160	5.9	10.8	1.33	59[c]	78.1	2.29
A2-37[b]	0.2986	5.9	10.3	1.33	2460	2.57	0.16
A2-38[b]	0.3012	5.9	10.3	1.33	1523	4.87	0.26

Note:
- [a] Severe bending present along the row of rivets.
- [b] Tests with near equal length cracks
- [c] Rivet failure occured before fatigue failure.

Method A No bending ($\gamma = 0.0$)

Method B Strength of materials estimate of bending ($\gamma = 3.0$)

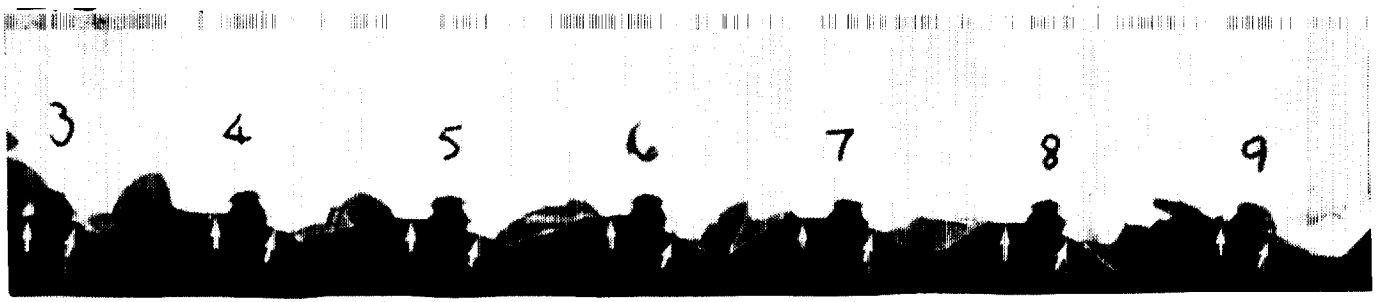

Figure 1. The MSD cracking which developed along the upper row of rivets in the Aloha Airlines Boeing 737-200.

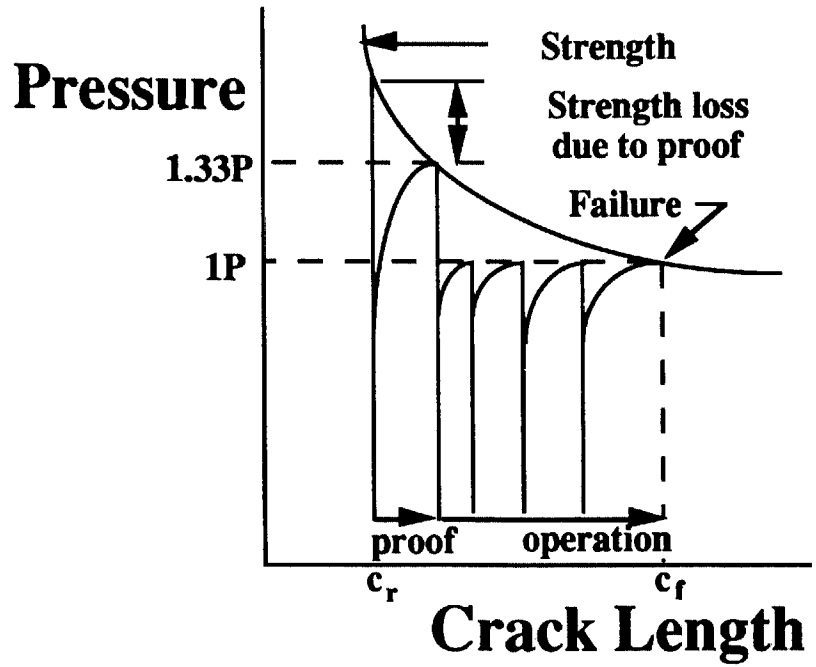

Figure 2a. Proof test logic for fuselage structures.

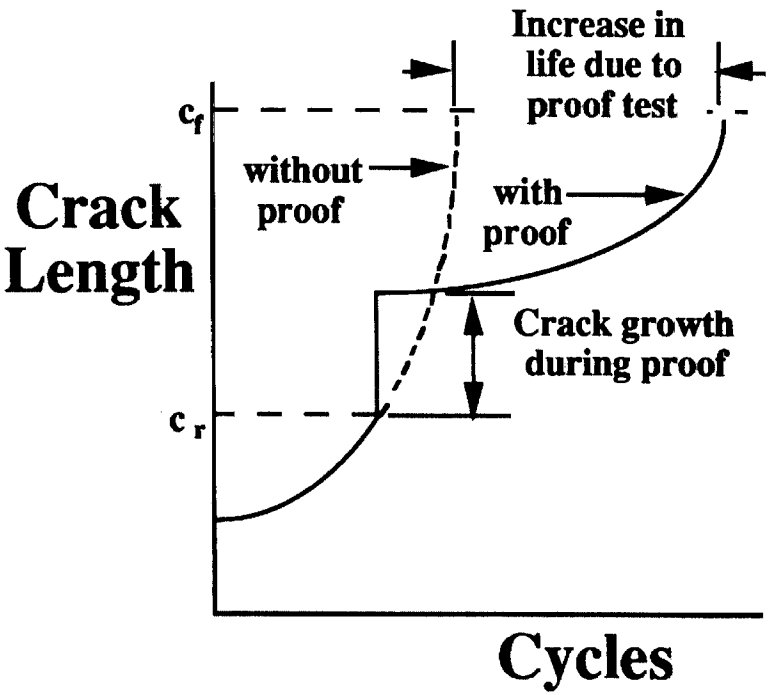

Figure 2b. Effect of proof test on life.

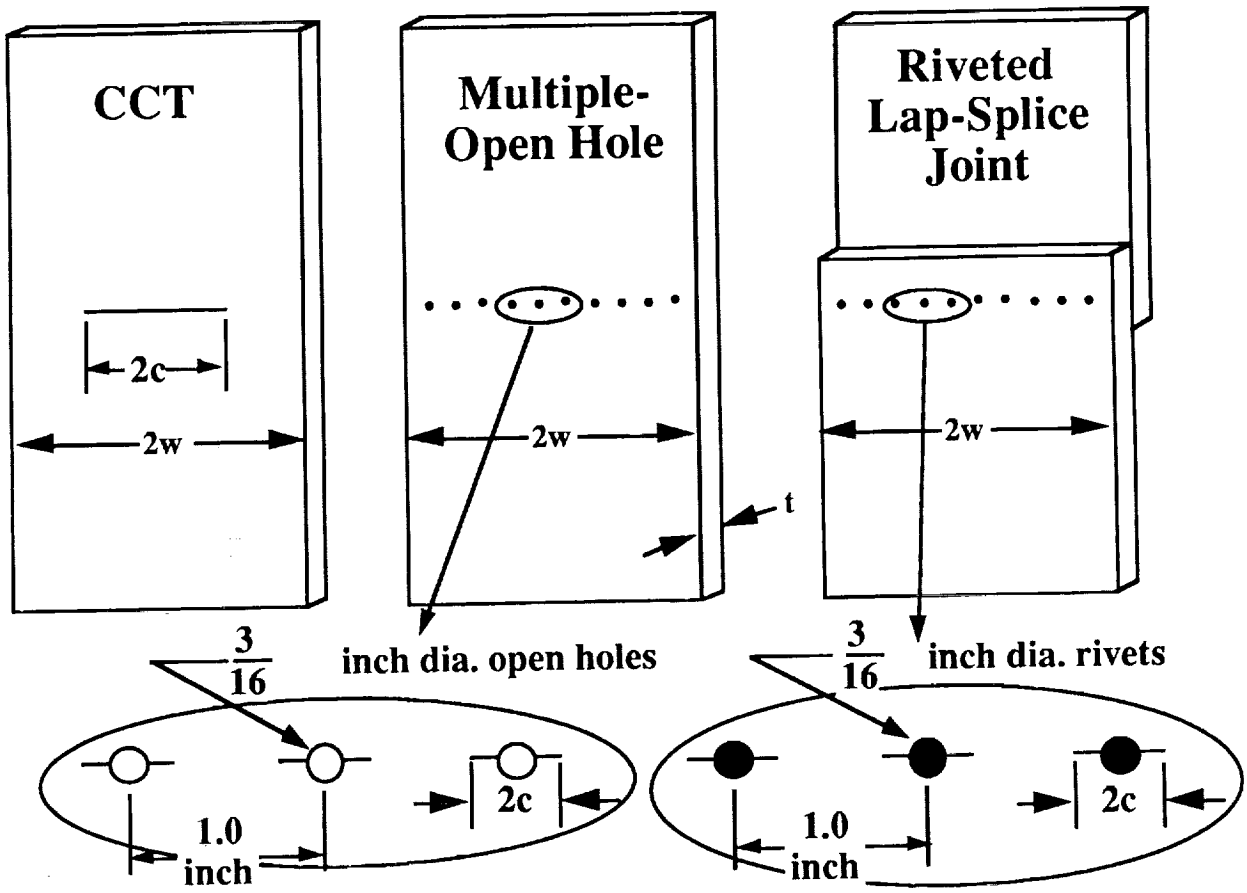

Figure 3. Specimen configurations used in the proof test evaluation.

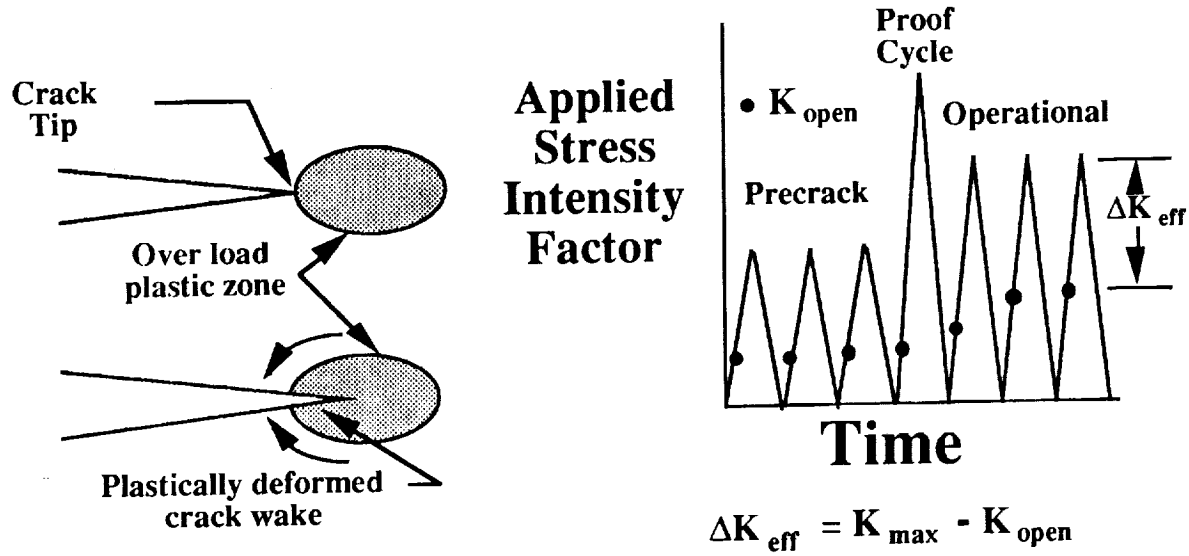

Figure 4. The plasticity induced fatigue crack closure and the effective stress intensity factor.

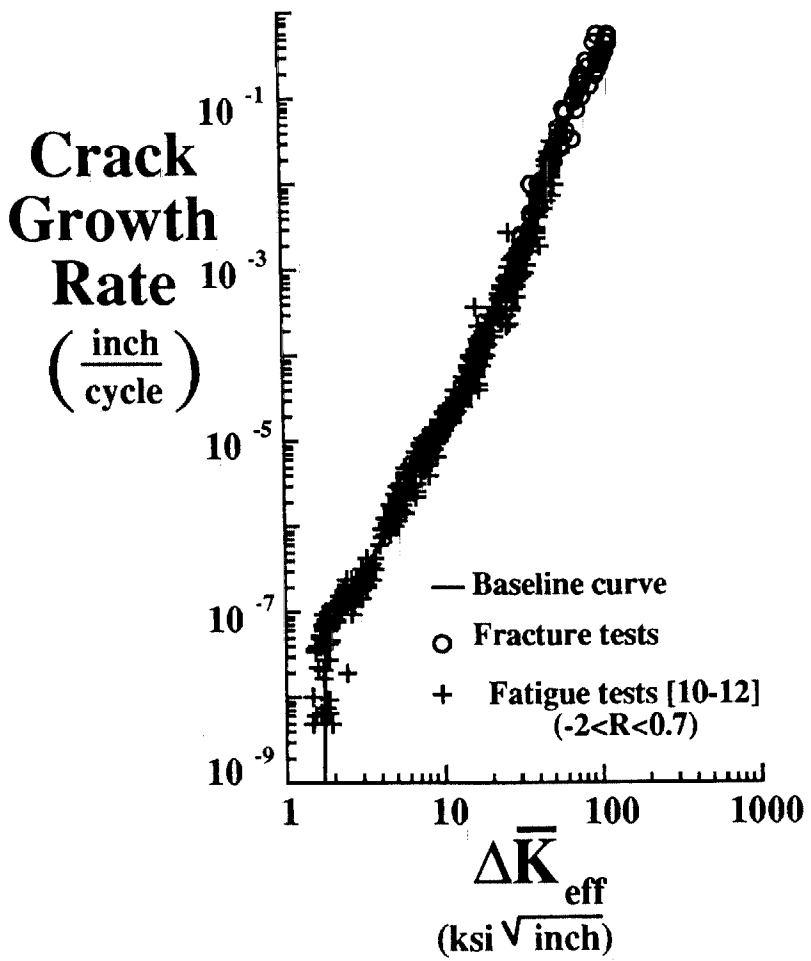

Figure 5. The effective stress intensity factor-crack growth rate behavior of the 2024-T3 aluminum alloy for thicknesses of 0.071-0.090 inches.

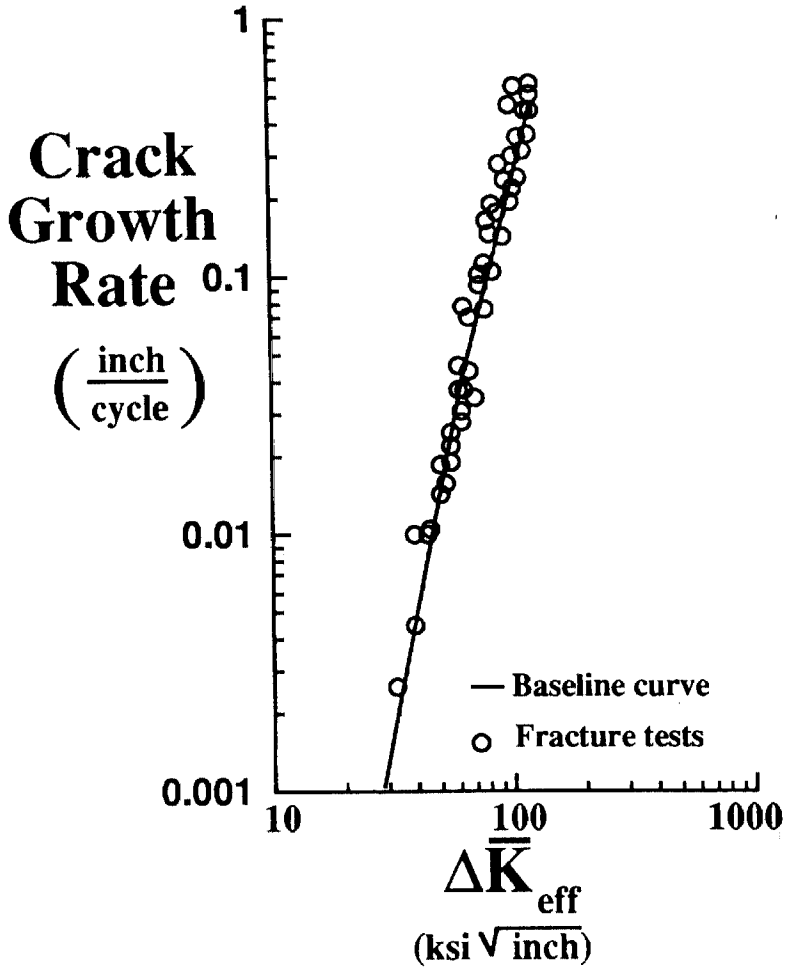

Figure 6. The correlation of the baseline fatigue crack growth rate data and the stable crack extension of fracture tests.

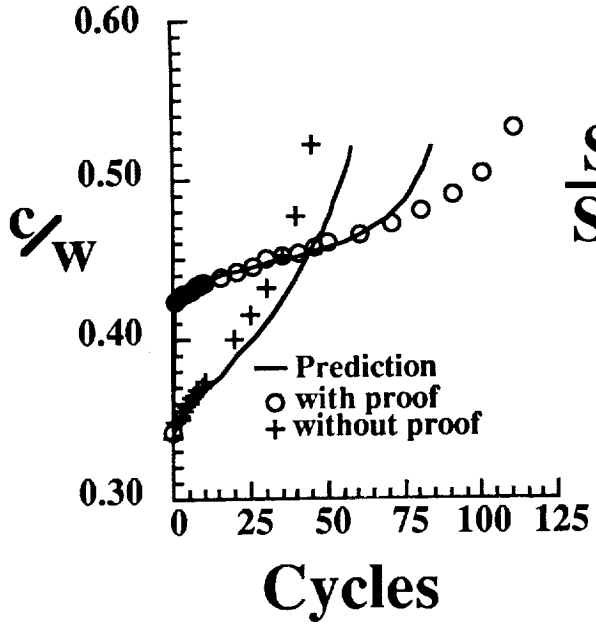

Figure 7a. Comparison of experimental and predicted crack growth lives for a CCT configuration with and without a 1.33 proof cycle.

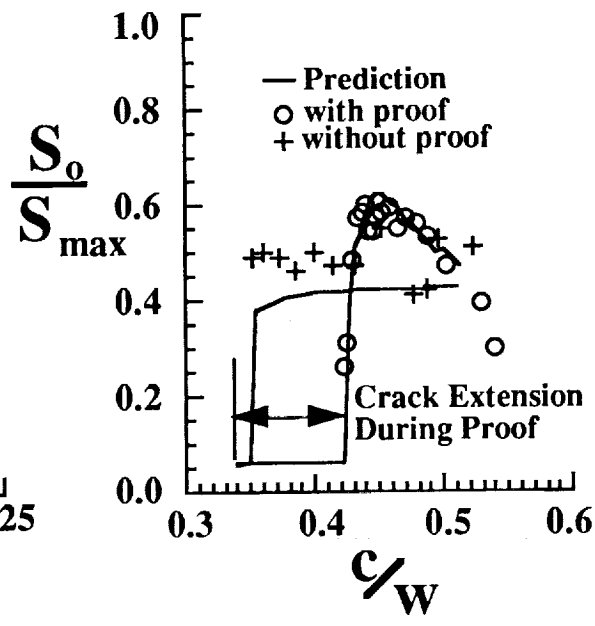

Figure 7b. Comparison of experimental and predicted crack opening stresses for a CCT configuration with and without a 1.33 proof cycle.

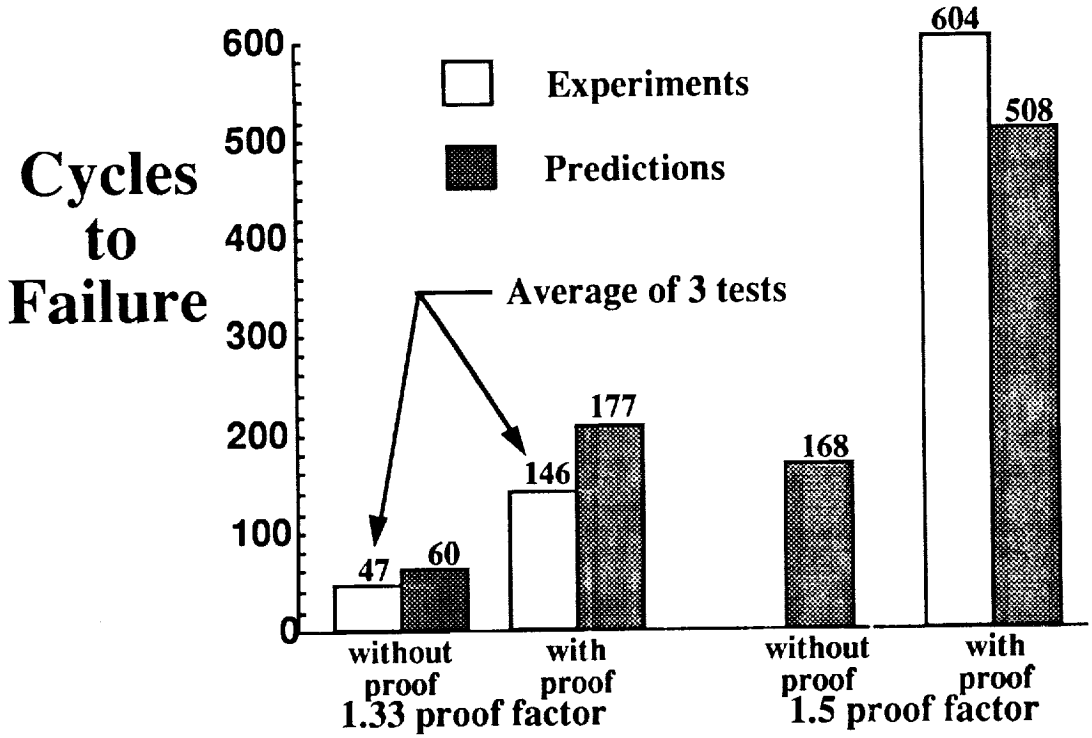

Figure 8. Comparison of fatigue life after proof for various proof factors for tests conducted at a stress level of about 11.5 ksi.

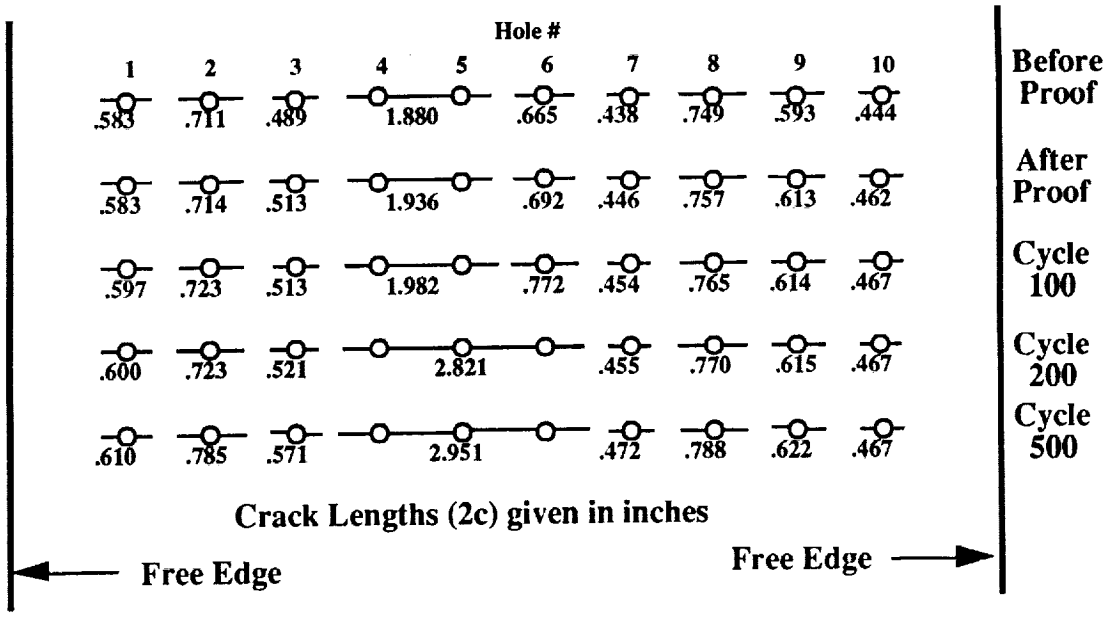

Figure 9. Progression of crack growth in open hole specimen A2-06 before and after the application of a 1.33 proof stress (541 cycles to failure).

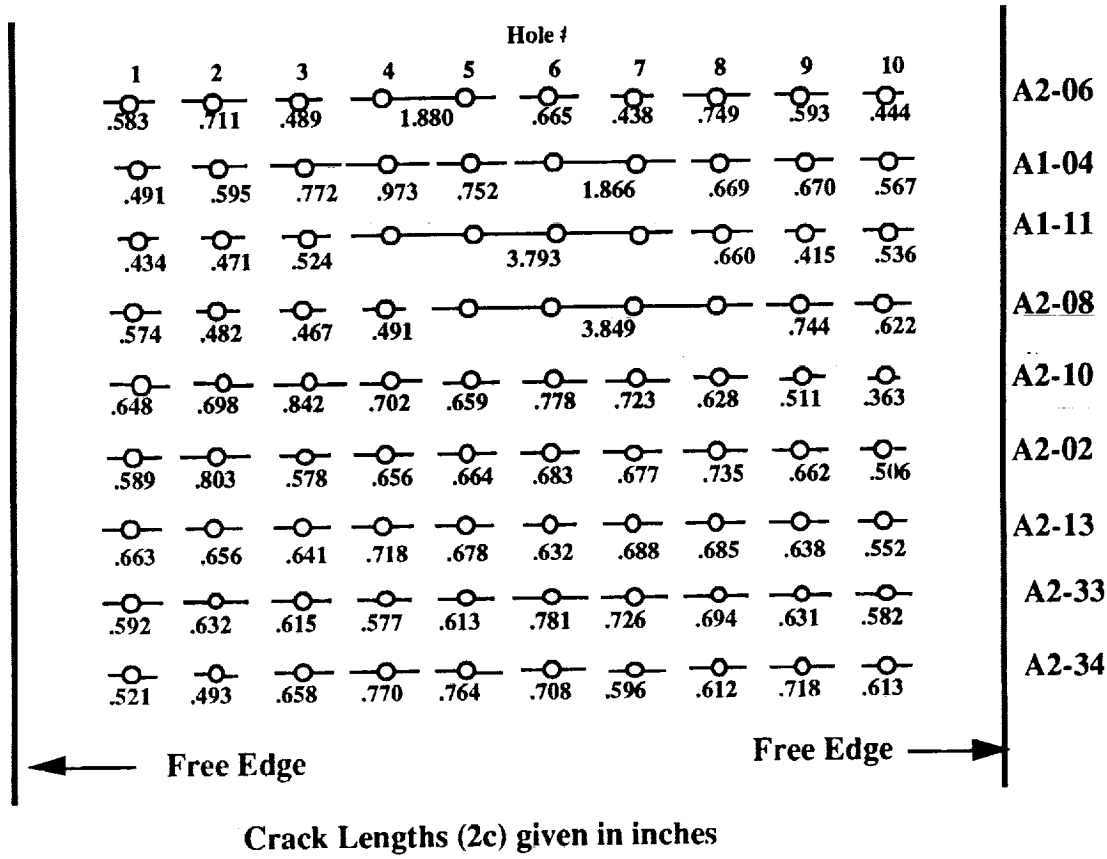

Figure 10. The crack length distributions prior to the application of the proof stress or at the start of the fatigue tests for the multiple-open hole specimens.

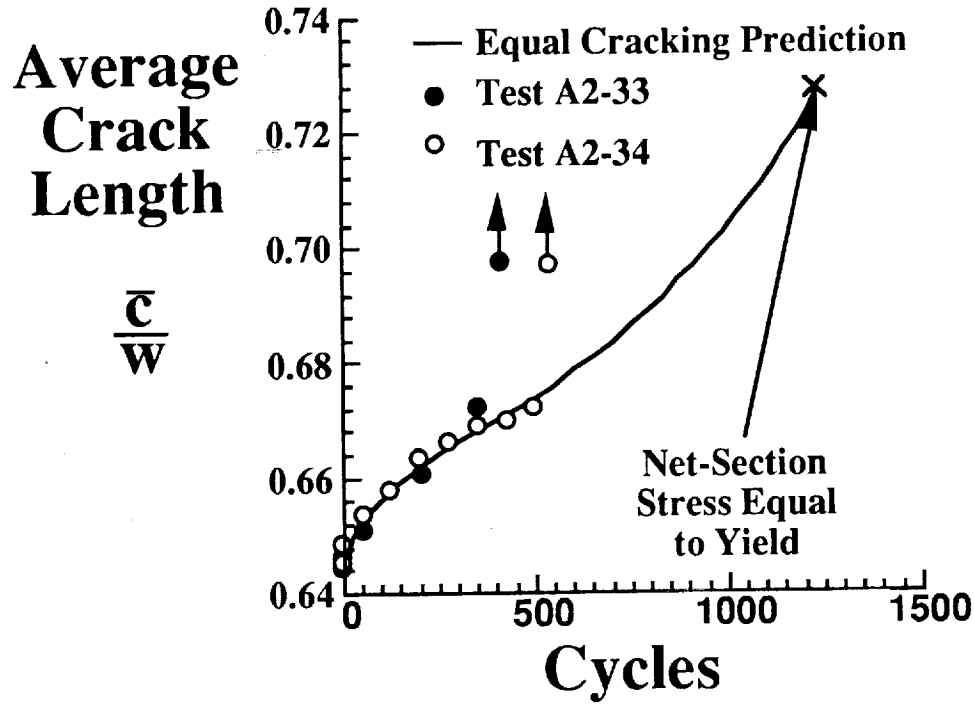

Figure 11. Experimental and predicted crack length against cycle behavior for two identical single proof cycle (1.33 proof factor) fatigue tests of multiple-open hole specimens with nearly equal cracking at each hole.

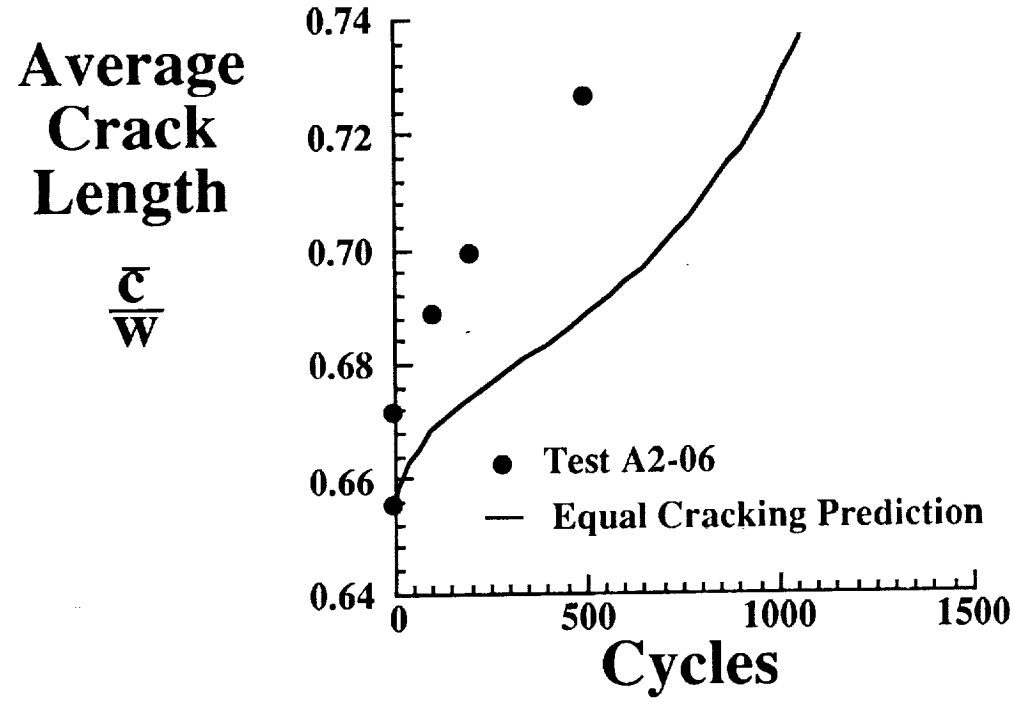

Figure 12. Experimental and predicted crack length against cycle behavior for a single proof cycle (1.33 proof factor) fatigue test of a multiple-open hole specimen with unequal cracking and crack link-up.

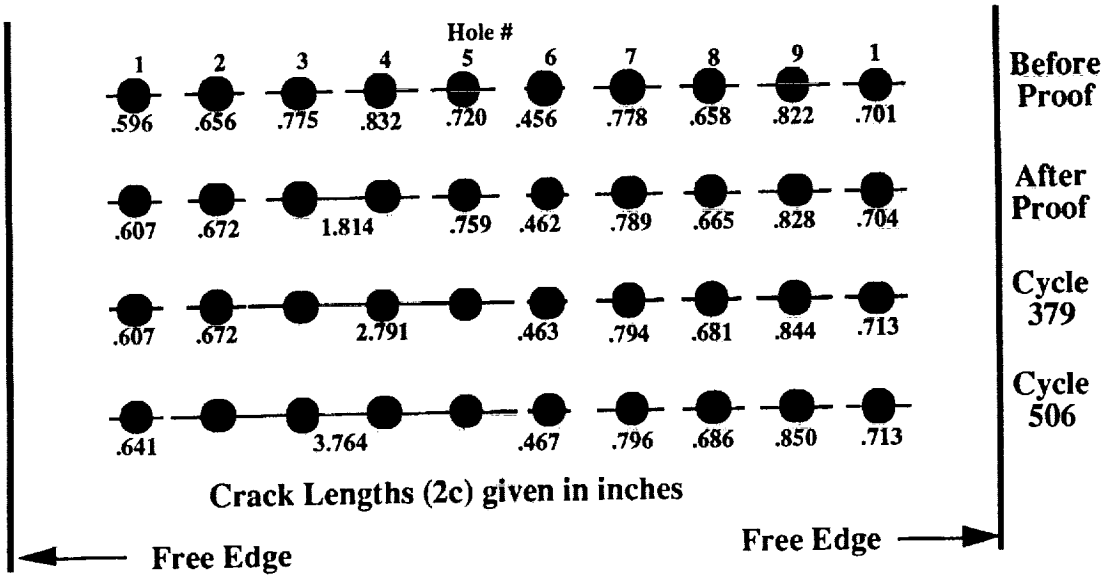

Figure 13. Progression of crack growth in the riveted lap-splice specimen A1-12 before and after the application of a 1.33 proof stress.

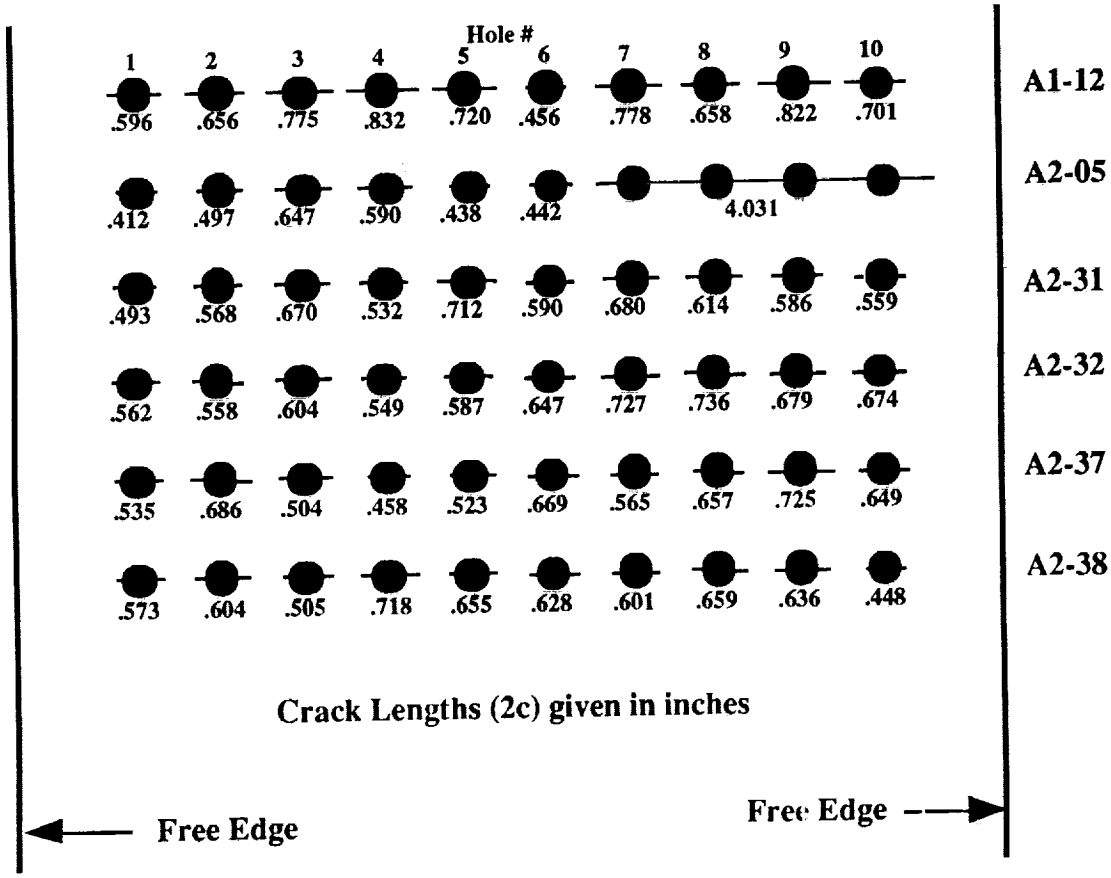

Figure 14. The crack length distributions prior to and immediately following the application of the 1.33 proof stress for the riveted lap-splice specimens.

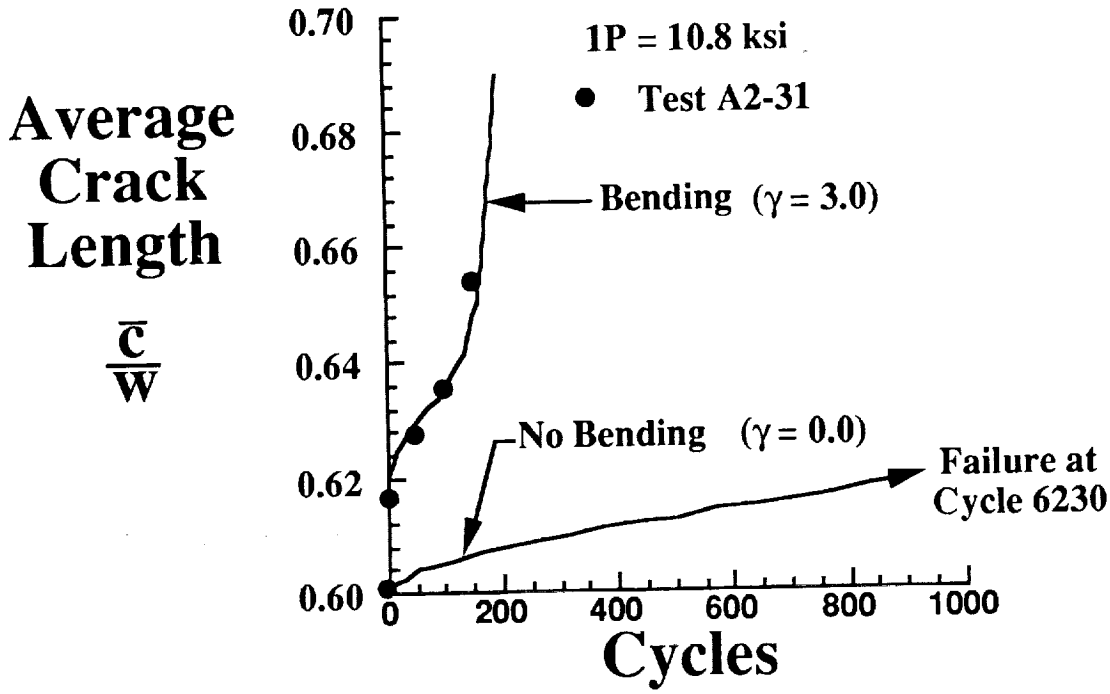

Figure 15. Experimental and predicted crack length against cycle behavior for a single proof cycle (1.33 proof factor) fatigue test of a riveted lap-splice joint specimen that exhibited severe bending.

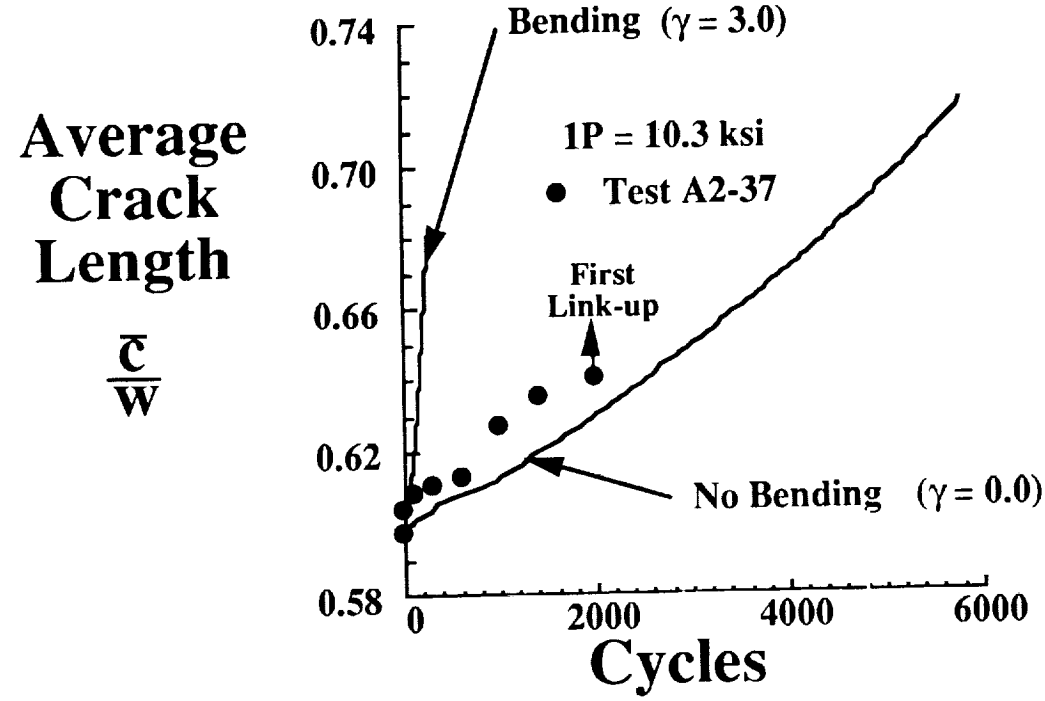

Figure 16. Experimental and predicted crack length against cycle behavior for a single proof cycle (1.33 proof factor) fatigue test of a riveted lap-splice joint specimen that exhibited very little bending.

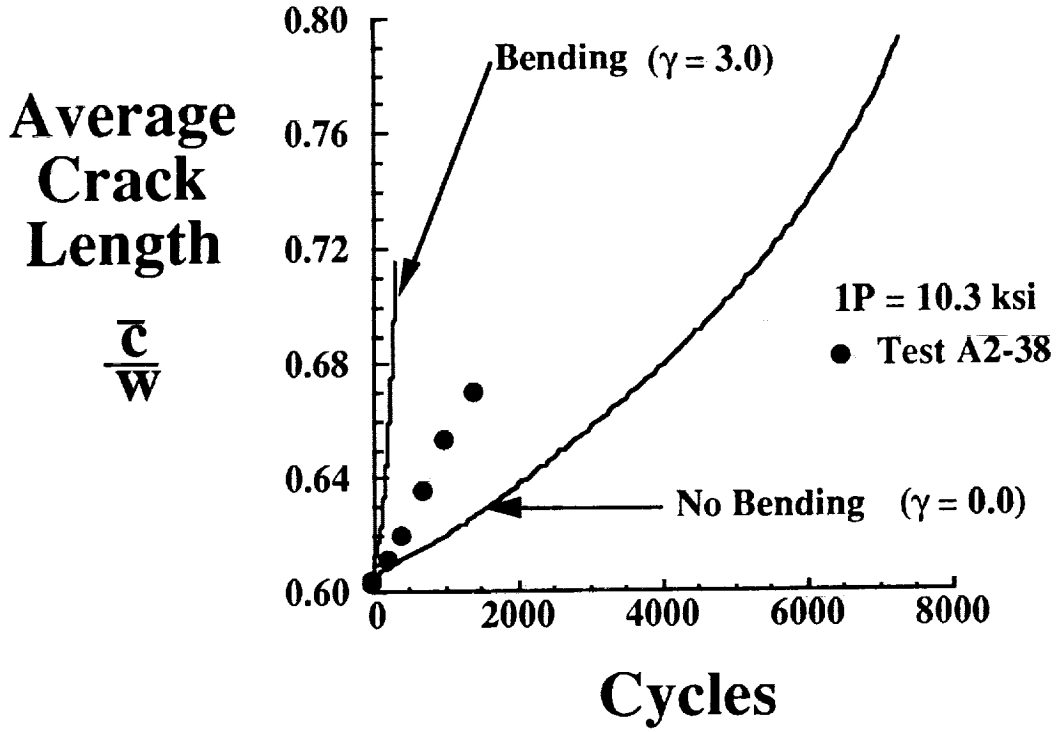

Figure 17. Experimental and predicted crack length against cycle behavior for a single proof cycle (1.33 proof factor) fatigue test of a riveted lap-splice joint specimen that exhibited moderate bending.

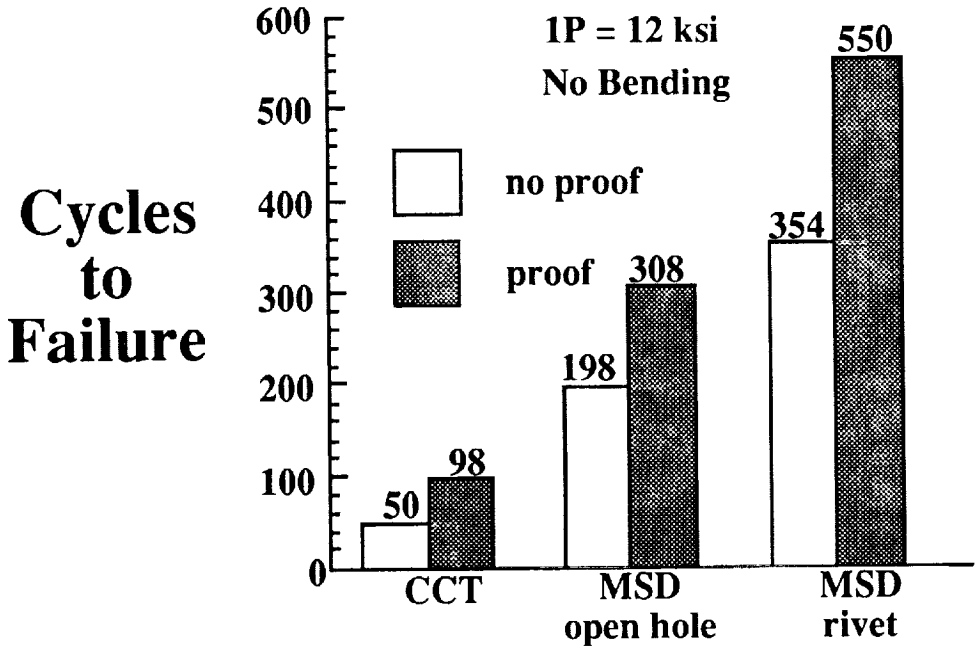

Figure 18. Predicted effect of proof stress on life for the CCT, open hole, and riveted lap-splice specimens without bending (1P = 12 ksi, 1.33 proof factor).

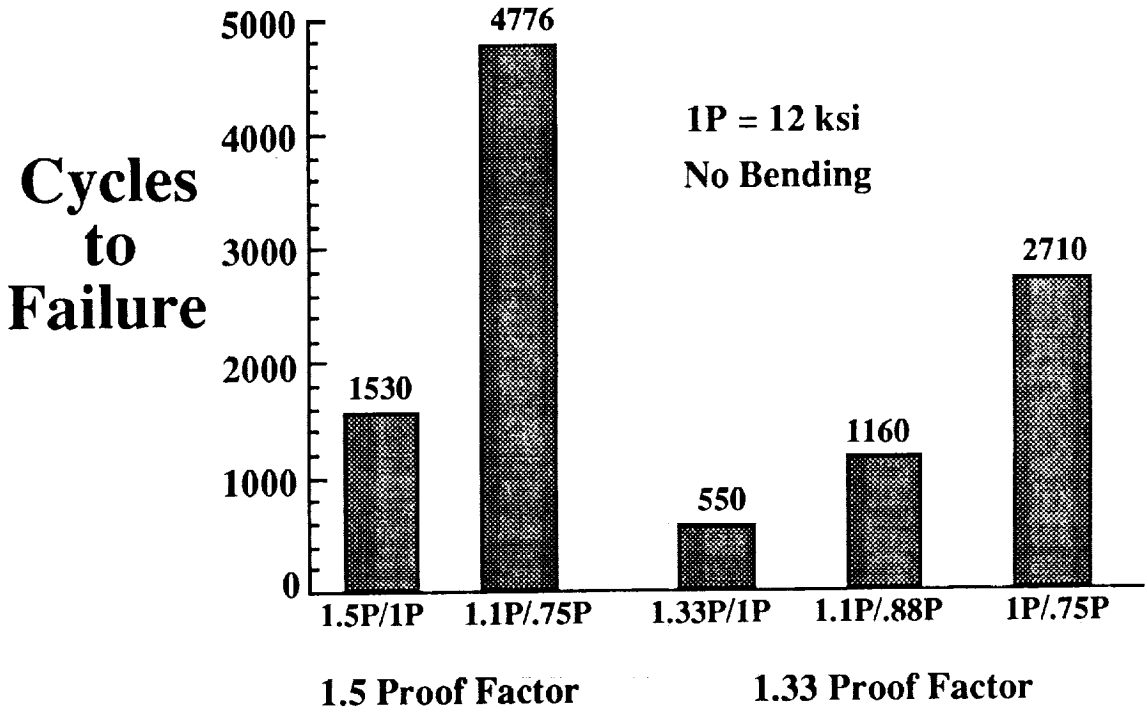

Figure 19. Predicted cycles to failure for the riveted lap-splice joint configuration, without bending, with cracks just critical for 1.5 and 1.33 proof factors and subjected to various operating conditions (proof stress/operational stress).

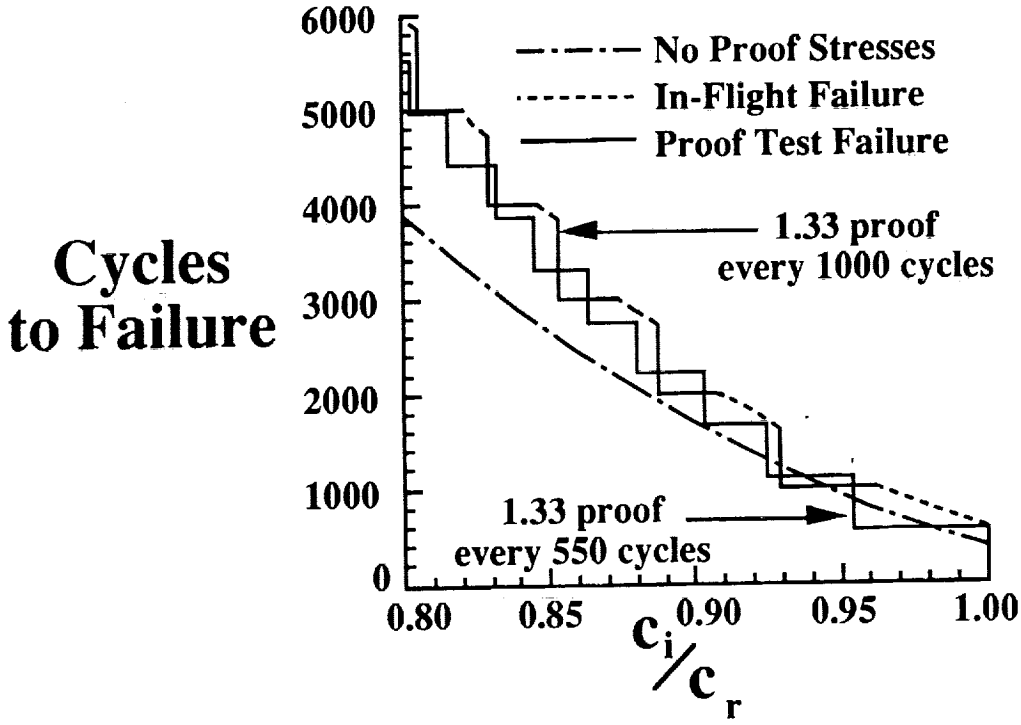

Figure 20. Predicted cycles to failure as a function of initial crack length for a riveted lap-splice joint, assuming no bending, subjected to an operational stress of 1P=12.0 ksi and a 1.33 proof factor applied every 550 or 1000 cycles.

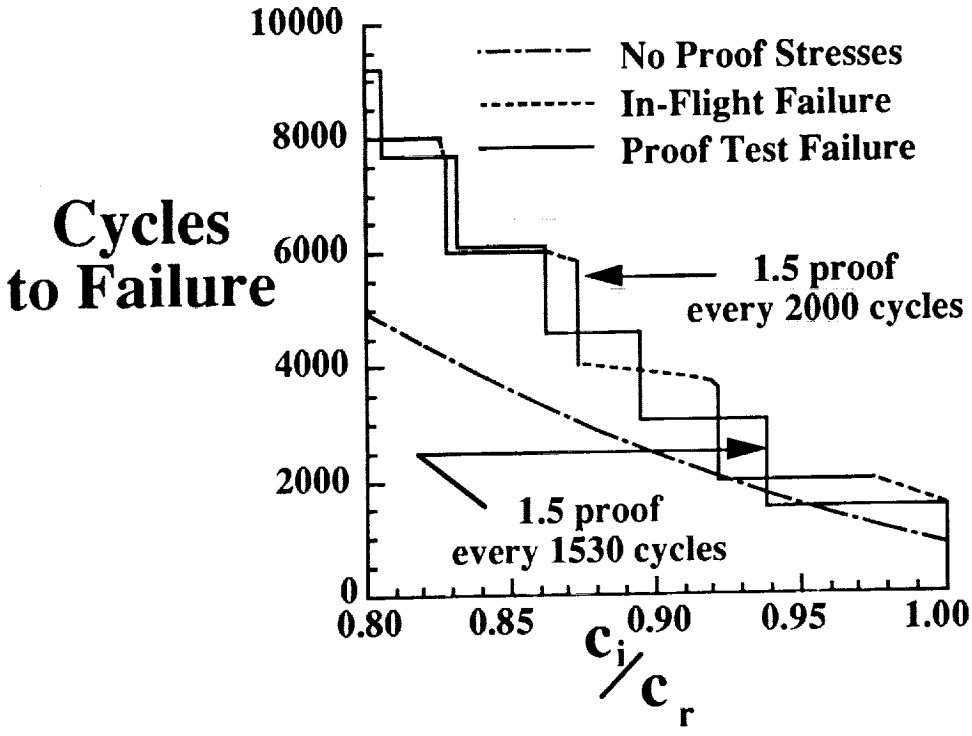

Figure 21. Predicted cycles to failure as a function of initial crack length for a riveted lap-splice joint, assuming no bending, subjected to an operational stress of 1P=12.0 ksi and a 1.5 proof factor applied every 1530 or 2000 cycles.

NASA
National Aeronautics and Space Administration

Report Documentation Page

1. Report No.	2. Government Accession No.	3. Recipient's Catalog No.
NASA TM-101675		

4. Title and Subtitle

An Evaluation of the Pressure Proof Test Concept for Thin Sheet 2024-T3

5. Report Date

April 1990

6. Performing Organization Code

7. Author(s)

D. S. Dawicke, C. C. Poe, Jr., J. C. Newman, Jr., and C. E. Harris

8. Performing Organization Report No.

10. Work Unit No.

505-63-01-05

9. Performing Organization Name and Address

NASA Langley Research Center
Hampton, VA 23665-5225

11. Contract or Grant No.

13. Type of Report and Period Covered

Technical Memorandum

12. Sponsoring Agency Name and Address

National Aeronautics and Space Administration
Washington, DC 20546

14. Sponsoring Agency Code

15. Supplementary Notes

D. S. Dawicke: Analytical Services & Materials, Inc., Hampton, Virginia
C. C. Poe, Jr., J. C. Newman, Jr., and C. E. Harris: Langley Research Center, Hampton, Virginia

16. Abstract

The concept of pressure proof testing of fuselage structures with fatigue cracks to insure structural integrity was evaluated from a fracture mechanics viewpoint. A generic analytical and experimental investigation was conducted on uniaxially loaded flat panels with crack configurations and stress levels typical of longitudinal lap splice joints in commercial transport aircraft fuselage. The results revealed that the remaining fatigue life after a proof test was longer than that without the proof test because of crack growth retardation due to increased crack closure. However, based on a crack length that is slightly less than the critical value at the maximum proof test stress, the minimum assured life or proof test interval must be no more than 550 pressure cycles for a 1.33 proof factor and 1530 pressure cycles for a 1.5 proof factor to prevent in-flight failures.

17. Key Words (Suggested by Author(s))	18. Distribution Statement
Proof tests Multi-site damage Fatigue Life predictions	Unclassified - Unlimited Subject Category - 39

19. Security Classif. (of this report)	20. Security Classif. (of this page)	21. No. of pages	22. Price
Unclassified	Unclassified	31	A03